

# Sub-micron particle dewatering using hydrocyclones

S. Pasquier, J.J. Cilliers\*

Department of Chemical Engineering, UMIST, P.O. Box 88, Manchester M60 1QD, UK

## Abstract

Hydrocyclones are used for dewatering of solid–liquid suspensions in many industries. Generally, however, large diameter cyclones are used and their application is restricted to large ( $>25\ \mu\text{m}$ ) particles. Small diameter (10 mm) hydrocyclones have the potential to be applied to fine particle ( $<10\ \mu\text{m}$ ) suspensions and, in particular, to collect the sub-micron fraction. This is due to the very small cutsizes that are achieved in these cyclones. In order to apply these small hydrocyclones industrially, knowledge of the range of their classification performance is required. It is found that these cyclones exhibit a fish-hook partition curve, and a high bypass fraction. The very small cutsize ( $<5\ \mu\text{m}$ ) and the relatively large bypass makes the effective collection of sub-micron particles possible. While in most hydrocyclone applications it is found that the bypass fraction equals the water recovery to the underflow, in 10 mm hydrocyclones the bypass fraction is considerably larger than the water recovery. This results in a high particle recovery to the underflow, as well as low water recovery, resulting in a high concentration ratio. Results will be presented to show the separation performance of different hydrocyclone outlet configurations and pressure drops. A general model will be presented that describes the fish-hook and that gives an explanation for its origin. It will be shown that 10 mm hydrocyclones yield a new operating regime for their application to sub-micron solid–liquid separation, as a result of high solids recoveries and low water recoveries. © 2000 Elsevier Science B.V. All rights reserved.

*Keywords:* Sub-micron particle; Hydrocyclones; Solid–liquid suspensions

## 1. Introduction

Hydrocyclones are used for dewatering of solid–liquid suspensions in many industries. Generally, however, large diameter cyclones are used and their application is restricted to large ( $>25\ \mu\text{m}$ ) particles. Small diameter (10 mm) hydrocyclones have the potential to be applied to fine particle ( $<10\ \mu\text{m}$ ) suspensions and, in particular, to collect the sub-micron fraction, due to the very small cutsizes that are achieved in these cyclones.

Previously, 10 mm hydrocyclones have been used successfully for dewatering yeast [1]. This illustrated that low density particles in a narrow size range can be collected in the short residence time in the cyclone. Detailed information about the size dependency of the dewatering in 10 mm cyclones has not been reported.

To describe the solids recovery, the size classification performance is required. It is found that these small cyclones exhibit a fish-hook partition curve [2], and have a high bypass fraction. A large bypass is undesirable for efficient classification, however yields high recoveries of solids. While in most hydrocyclone applications it is found that the bypass

fraction equals the water recovery to the underflow, in 10 mm hydrocyclones the bypass fraction is considerably larger than the water recovery. This results in a high particle recovery to the underflow, as well as low water recovery, resulting in a high concentration ratio, and effective solid–liquid separation.

In this study, the separation performance of 10 mm cyclones with a range of outlet dimensions will be evaluated. To describe the classification performance, a general model will be presented that describes the fish-hook and that gives an explanation for its origin. In particular, the relationship between the bypass fraction and other performance indicators will be explored.

## 2. Background

### 2.1. Solids recovery: the partition curve

The partition curve (also called a performance curve, efficiency curve or Tromp curve) shows the fraction of material of a specific size,  $d$ , in the feed to a classifier that reports to the coarse product stream. In the case of hydrocyclones, this is the underflow. The graph is usually plotted on a log-linear scale to emphasize the fine particle sizes.

\* Corresponding author. Tel.: +44-161-200-4353;  
fax: +44-161-2004399.  
E-mail address: j.j.cilliers@umist.ac.uk (J.J. Cilliers).

For any particle size  $d$ , the partition number,  $P(d)$ , is calculated from

$$P(d) = \frac{Uu(d)}{Ff(d)} \quad (1)$$

where  $U$  and  $F$  are the mass flow rates of solids and  $u(d)$  and  $f(d)$  are the fractions of particle size  $d$  in the underflow and feed streams, respectively. For hydrocyclones, the partition number for small particle sizes generally is not zero, but asymptotes to a particular value. This value is commonly referred to as the bypass,  $B_p$ , which corresponds to the fraction of particles in the feed that bypasses the classification.

If the experimentally measured partition curve is monotonic, it can be *corrected* to asymptote to zero at small particle sizes by scaling the partition number. The relationship between the experimental partition curve,  $P(d)$ , the corrected partition curve,  $C(d)$ , and the bypass,  $B_p$ , is given by

$$C(d) = \frac{P(d) - B_p}{1 - B_p} \quad (2)$$

Corrected partition curves are generally modelled using sigmoidal functional forms. A commonly used equation is the Rosin-Rammler [3,4]

$$C(d) = 1 - \exp(-0.693(d/d_{50c})^m) \quad (3)$$

Half of the particles of the corrected cut size,  $d_{50c}$ , will report to the coarse stream, and  $m$  indicates the sharpness of separation. Other equation forms, such as the exponential sum [5] have also been used.

## 2.2. Modelling the bypass, $B_p$

It is generally assumed [3,6–8] that the bypass is independent of particle size and equals the water recovery from the feed to the underflow,  $R_f$ . Austin and Klimpel [9] argue that there is no fundamental reason why, in general, this should be so, and show data where the bypass is clearly not equal to the water recovery.

Svarovsky [10] and Braun and Bohnet [11] assume that the bypass equals the fraction of the feed slurry reporting to the underflow. This assumption is not commonly used, but is a close approximation to the water recovery at low feed solids concentrations and is more readily measured.

## 2.3. Modelling the fish-hook

When the partition curve displays a fish-hook, the simple ‘correction’ approach cannot be applied, and a more complex model is required.

Eq. (2) can be rearranged to yield

$$P(d) = C(d) + B_p [1 - C(d)] \quad (4)$$

This indicates the observed partition curve,  $P(d)$ , can be considered as consisting of two components, a corrected partition curve,  $C(d)$ , and an inverse partition curve,  $1 - C(d)$ ,

multiplied by the bypass,  $B_p$ . For a monotonically decreasing partition curve the two  $C(d)$  terms are the same. However, this need not be so and, by changing the form of the second term, a fish-hook shape can be reproduced.

Finch [2] first used this concept and considered the second term,  $a(d)$ , as a size dependent entrainment function that increases as the particle size decreases.

$$P(d) = C(d) + a(d) \quad (5)$$

where:

$$a(d) = R_f \left( 1 - \frac{d}{d_0} \right)$$

The value of  $d_0$  represents the largest particle size affected by the fish-hook. It is assumed that the bypass equals the water recovery. Del Villar and Finch [12] modified this function, arguing that the contribution of the entrainment term is probabilistic and not truly additive. Eq. (5) then becomes

$$P(d) = a(d) + [1 - a(d)]C(d) \quad (6)$$

which can be rearranged as

$$P(d) = C(d) + a(d)[1 - C(d)] \quad (7)$$

where

$$a(d) = R_f(1 - d/d_0) \quad \text{for } d < d_0$$

$$a(d) = 0 \quad \text{for } d > d_0$$

Del Villar and Finch also assumed that the experimental curve asymptotes to the water recovery at the finest particle sizes. Roldan-Villasana et al. [13] find that this later model is an improvement over that of Finch, particularly in the modelling of coarse particle sizes. They argue that both these models suffer the disadvantage of not having a defined derivative, and are able to describe only shallow fish-hooks.

An alternative is given by Hodouin et al. [14] who consider the feed as being split into two fractions. A fraction equal to the water recovery is classified by entrainment. This entrainment function,  $C^*(d)$ , has the same mathematical form as the classification function,  $C(d)$ . The coarse product of the entrainment is recombined with the remainder of the feed and classified by  $C(d)$ . The coarse product of the classification and the fine product of the entrainment functions are combined as the final product.

Mathematically, this is represented as

$$P(d) = R_f [1 - C(d)] + C^*(d) [R_f C(d) + (1 - R_f)] \quad (8)$$

This can be re-arranged as

$$P(d) = C(d) + R_f [1 - C^*(d)] [1 - C(d)] \quad (9)$$

which shows that the assumption of the bypass equalling the water recovery is made, and that the second term consists of the product of two inverted partition functions.

#### 2.4. A general partition curve model

It can be seen that the three models described [1,12,14] have a similar form that can be represented by

$$P(d) = C(d) + B_p [1 - E(d)] \quad (10)$$

Thus the observed partition curve,  $P(d)$ , can be interpreted as a combination of a classification partition curve,  $C(d)$ , and a dispersion function  $E(d)$ , affecting a fraction,  $B_p$ , of the feed to the cyclone. The dispersion will be particle size dependent, and can be expected to increase as the particles become smaller.

It is useful if the mathematical form of the dispersion function is chosen to be the same as that of the classification function. When the cutsize and sharpness of  $E(d)$  are the same as for  $C(d)$ , the equation reverts to that for a partition curve without a fish-hook. If they are not equal, fish-hooks of any depth and breadth can be modelled.

If the dispersion and classification functions are both modelled using the Plitt/Reid form, then the following expression is produced [16]:

$$P(d) = (1 - \exp(-0.693 (d/d_{50\text{class}})^{m_{\text{class}}})) + B_p (\exp(-0.693 (d/d_{50\text{disp}})^{m_{\text{disp}}})) \quad (11)$$

The classification is defined by the classification cutsize,  $d_{50\text{class}}$ , and the classification sharpness,  $m_{\text{class}}$ , and the dispersion by the dispersion cutsize,  $d_{50\text{disp}}$ , and the dispersion sharpness,  $m_{\text{disp}}$ . Note that in this general model the bypass,  $B_p$ , is not assumed to be equal to the water recovery. As previously noted, this assumption is not always valid, although it is in many cases a good approximation. Turbulent dispersion or other factors such as chemical dispersants [15] can affect the bypass. As will be shown later, the bypass can also be significantly larger than the water recovery, indicating that the conventional interpretation that an equivalent fraction of the feed solids follows the water to the underflow is not always correct.

#### 2.5. Quantifying dewatering performance

Quantifying the dewatering performance requires two values: the recovery of solids from the feed to the underflow,  $R_s$ , and the concentration ratio,  $C$ , the ratio of the concentrations of the underflow to the feed. It can be noted that the ratio of these two values, in turn, yields the volumetric recovery of suspension to the underflow,  $R_v$ , also called the flow ratio.

$$R_v = \frac{R_s}{C} \quad (12)$$

Other measures have been used to describe dewatering efficiency. The clarification efficiency,  $E_c$ , is related to the flow ratio,  $R_v$ , and concentration ratio,  $C$ , by the following relationships:

$$E_c = (C - 1) \frac{R_v}{(1 - R_v)} \quad (13)$$

$$E_c = \frac{(R_s - R_v)}{(1 - R_v)} \quad (14)$$

It can be seen that the clarification efficiency is equivalent to the solids recovery corrected using the volumetric recovery (cf. Eq. (2)).

### 3. Experimental method

A single 10 mm ceramic solid–liquid hydrocyclone, supplied by Richard Mozley (UK), was used for the experiments. A Mono pump was used to feed the system and a bypass valve was used for pressure control. Two vortex finders, of diameter 2.0 and 3.2 mm, and two spigots, with diameters 1.0 and 2.0 mm, were used, in their four combinations, as a two-level full factorial experimental programme. This allows the observed responses to be modelled as a combination of linear and interaction terms of the two variables.

The solid feed material was silica flour with a median size of 8.5  $\mu\text{m}$ , supplied by Hepworth Minerals (UK). The feed concentration was approximately 35 g/l, which is low enough to not affect the viscosity or volumetric recovery significantly. The feed pressure was held constant at 4.0 bar, with both outlets open to the atmosphere. In a series of experiments previously described [16], a 2 mm vortex finder and 1 mm spigot was used and the pressure varied between 2.0 and 4.0 bar.

Samples were taken from the feed and simultaneously from the two product streams. A proportion was dried to determine the solids concentration. Overall mass balance discrepancies were less than 2%.

A sub-sample of each stream was size analysed using a Malvern Mastersizer without drying, to eliminate agglomeration. It was found, by comparing the experimentally measured solids recovery with the solids recovery estimated from the three fractional size analyses, that results below 0.3  $\mu\text{m}$  were generally unreliable and were not used for modelling. In the region of the partition curve where the fish-hook was observed, this discrepancy was generally less than 5%, confirming the validity of the data. In the case of the 2 mm vortex finder and 2 mm spigot, data to 0.2  $\mu\text{m}$  was used, since the fish-hook only appeared at very fine sizes and the data was good.

The five parameters of the general equation (the classification and dispersion cutsizes and sharpnesses, respectively, and the bypass) were simultaneously estimated by minimising the sum-of-errors difference between the observed and estimated partition values, while constraining the estimation to predict the experimentally measured solids recovery.

Table 1  
Experimental results for overall hydrocyclone performance

Spigot (mm)	Vortex finder (mm)	Solids recovery, $R_s$ (%)	Volumetric recovery, $R_v$ (%)	Water recovery, $R_f$ (%)	Concentration ratio, $C$	Flow rate, $Q$ (ml/s)
1.0	3.2	64.8	5.4	4.1	12.2	62.2
1.0	2.0	80.1	15.9	13.8	5.0	35.6
2.0	3.2	77.0	17.7	15.5	4.4	60.7
2.0	2.0	92.8	55.8	54.2	1.7	40.5

## 4. Results and discussion

### 4.1. Overall performance

The effect of the outlet dimensions on the overall hydrocyclone performance is summarised in Table 1.

The volumetric throughput,  $Q$ , is affected strongly by the vortex finder dimension, but is largely independent of the spigot size. In contrast, the recovery of solids to the underflow (total efficiency,  $R_s$ ) is significantly increased by a decrease in the vortex finder diameter and by an increase in the spigot diameter. These variables have an independent, equal and opposite effect on  $R_s$ , and their effect can be combined as a linear dependency on the difference in their diameters.

The volumetric recovery is significantly affected by the interaction between the outlet dimensions. The response can be described accurately as a function of the ratio of the outlet areas, i.e. the square of the ratio of their dimensions.

As noted, the concentration ratio of the underflow to feed streams is given by the ratio of the solids and volumetric recoveries and is therefore affected by their relative responses.

Thus, for example, doubling the vortex finder diameter will lead to a linearly proportional decrease in solids recovery, but will more than double the concentration ratio, due to the outlet area dependency of volumetric recovery. This is borne out by the data; increasing the vortex finder from 2 to 3.2 mm increases the concentration ratio from 5.0 to 12.2 (256%), while the solids and volumetric recoveries decrease by 20 and 66%, respectively.

The effect of inlet pressure on the separation performance of a 10 mm cyclone has been described previously [16]. As the inlet pressure is decreased, the concentration ratio decreases, due to the simultaneous decrease in the solids recovery and increase in the volumetric recovery. It can be noted that the effect of pressure is significantly smaller than the effect of outlet diameter changes; reducing the inlet pressure from 4 to 2 bar reduces the concentration ratio by only 15%, the solids recovery decreasing by 6.5% and the volumetric recovery increasing by 9.5%.

It is of interest to note that the changes in outlet diameters and the change in pressure affect the solids and volumetric recoveries in different ways. A change in outlet diameter is positively correlated with both solids and volumetric recov-

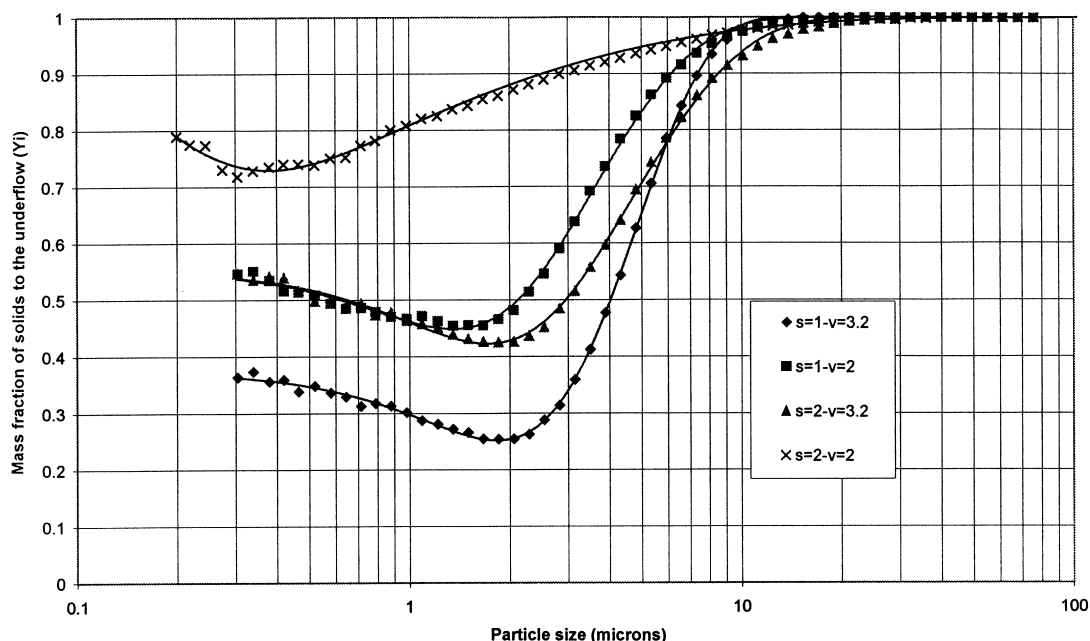


Fig. 1. Experimental (points) and fitted (solid lines) partition curves.

Table 2  
Experimental results for hydrocyclone classification performance

Spigot (mm)	Vortex finder (mm)	Classification cutsize, $d_{50\text{class}}$ ( $\mu\text{m}$ )	Dispersion cutsize, $d_{50\text{disp}}$ ( $\mu\text{m}$ )	Classification sharpness, $m_{\text{class}}$	Dispersion sharpness, $m_{\text{disp}}$	Bypass (%)
1.0	3.2	4.32	1.19	1.69	2.11	34.9
1.0	2.0	2.33	0.92	1.24	1.57	54.6
2.0	3.2	3.10	1.08	1.18	1.55	54.5
2.0	2.0	0.09	0.08	0.36	1.01	100.0

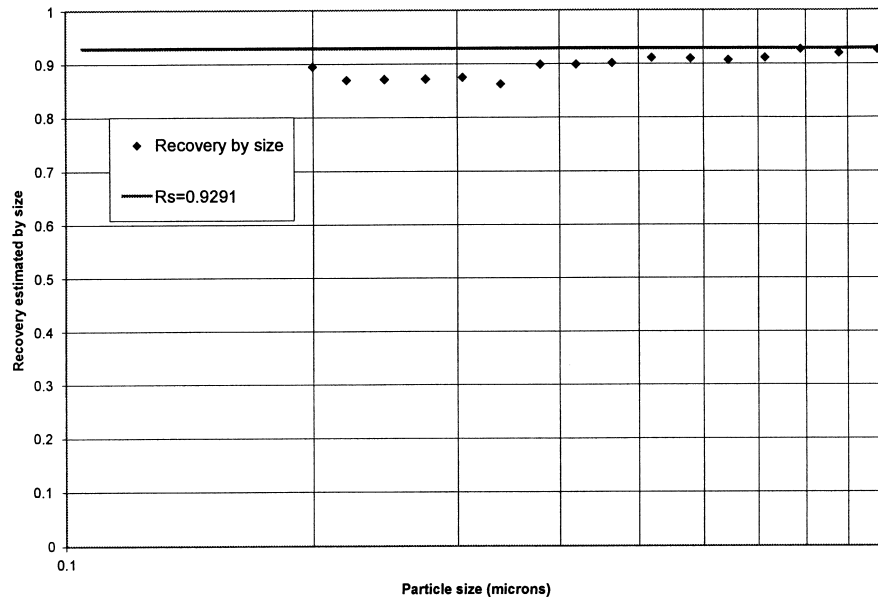


Fig. 2. Comparison of measured (line) and estimated (points) solids recovery.

ery, while a change in pressure has opposing effects on these responses.

#### 4.2. Classification performance

##### 4.2.1. Partition curves

Fig. 1 shows the partition curves for the four combinations of outlets. It can be noted that the fish-hook effect is pronounced and that the bypass is significant. The values of the classification parameters are given in Table 2. Fig. 1 further shows that Eq. (11) very closely describes the measured data, as indicated by the solid lines.

Fig. 2 shows the total recovery of solids estimated on a size-by-size basis for the 2 mm spigot and vortex finder experiment, for particles finer than 1  $\mu\text{m}$ , which is representative of all the tests. It can be seen that the recovery estimated for each size class is consistent with the overall mass balance.

The partition curves clearly show the reason for the high concentration ratios obtained in the 10 mm hydrocyclones. The partition curves indicate that essentially all particles coarser than 10  $\mu\text{m}$  are collected as well as, due to the high bypass, a significant fraction of the sub-micron material. It must be emphasised that the bypass is not related to either

the volumetric recovery or the water recovery, both of which are significantly lower than the bypass (cf. Tables 1 and 2). The bypass is effective at removing particles to the coarse product, but, as a result, the classification performance is rather poor.

The origin of the bypass fraction is not immediately apparent. It was previously suggested that the bypass is related to the turbulent dispersion of particles and therefore indicates the fraction of the solids that is subject to such turbulent dispersion [16]. In that case, it may be postulated that the bypass should be related to the flowrate through the hydrocyclone; this is clearly not the case.

## 5. Conclusions

The dewatering performance of 10 mm hydrocyclones with a range of outlet dimensions has been described. It has been found that these cyclones are able to produce high concentration ratios, due to the small cutsizes and high bypass fractions, coupled with a low volumetric recovery.

A general classification model was developed that accurately describes the fish-hook partition curve observed. It was found that the classification performance exhibited a

significant bypass, which, although it produces inferior classification, is valuable for solid–liquid separation. It was clear from the results that neither the water recovery nor the volumetric recovery determines the value of the bypass, both being significantly lower. The origin of the bypass is, as yet, inexplicable.

## References

- [1] J.J. Cilliers, S.T.L. Harrison, The application of mini-hydrocyclones in the concentration of yeast suspensions, *Chem. Eng. J.* 65 (1997) 21–26.
- [2] J.A. Finch, Modelling a fish-hook in hydrocyclone selectivity curves, *Powder Technol.* 36 (1983) 127–129.
- [3] L.R. Plitt, A mathematical model of the hydrocyclone classifier. *CIM Bull.* December (1976) 114–122.
- [4] K.J. Reid, Derivation of an equation for classifier performance curves, *Can. Metall. Q.* 10 (1971) 253–254.
- [5] A.J. Lynch, T.C. Rao, Modelling and scale-up of hydrocyclone classifiers. *Proc. 11th Int. Min. Proc. Congr., Cagliari, 1975*, pp. 245–269.
- [6] B.C. Flinchoff, L.R. Plitt, A.A. Turak, Cyclone modelling: a review of present technologies. *CIM Bull.* September (1987) 39–50.
- [7] L.G. Austin, R.R. Klimpel, P.T. Luckie, *Process Engineering of Size Reduction: Ball Milling*, SME of American Institute of Mining, Metallurgical and Petroleum Engineers, New York, 1984.
- [8] A.J. Lynch, *Mineral Crushing and Grinding Circuits: Their Simulation, Optimization, Design and Control*, Elsevier, Amsterdam, 1977.
- [9] L.G. Austin, R.R. Klimpel, An improved method for analyzing classifier data, *Powder Technol.* 29 (1981) 277–281.
- [10] L. Svarovsky, *Hydrocyclones*, Holt, Rinehart and Winston, London, 1992.
- [11] T. Braun, M. Bohnet, Influence of feed solid concentration on the performance of hydrocyclones, *Chem. Eng. Technol.* 13 (1990) 15–20.
- [12] R. Del Villar, J.A. Finch, Modelling the cyclone performance with a size dependant entrainment factor, *Miner. Eng.* 5 (1992) 661–669.
- [13] E.J. Roldan-Villasana, R.A. Williams, T. Dyakowski, The origin of the fish-hook effect in hydrocyclone separators, *Powder Technol.* 77 (1993) 243–250.
- [14] D. Hodouin, S. Caron, J.J. Grand, Modelling and simulation of a hydrocyclone desliming unit. *1st World Congress on Particle Technology, Nurnberg, Part IV, 1986*, pp. 507–522.
- [15] R.R. Klimpel, The influence of chemical dispersant on the sizing performance of a 24-in hydrocyclone, *Powder Technol.* 31 (1982) 255–262.
- [16] M. Frachon, J.J. Cilliers, A general model for hydrocyclone partition curves, *Chem. Eng. J.* 73 (1999) 53–59.